A search for circularly polarized emission from young exoplanets

C. R. Lynch,[1,2]⋆ Tara Murphy,[1,2] D. L. Kaplan,[3] M. Ireland[4] and M. E. Bell[2,5]

[1]*Sydney Institute for Astronomy, School of Physics, The University of Sydney, NSW 2006, Australia*
[2]*ARC Centre of Excellence for All-sky Astrophysics (CAASTRO), Sydney Institute for Astronomy, School of Physics,*
The University of Sydney, Sydney, NSW 2006, Australia
[3]*Department of Physics, University of Wisconsin–Milwaukee, Milwaukee, WI 53201, USA*
[4]*Research School for Astronomy & Astrophysics, Australia National University, Canberra, ACT 2611, Australia*
[5]*CSIRO Astronomy and Space Science, PO Box 76, Epping, NSW 1710, Australia*

ABSTRACT

We report the results of a 154 MHz survey to search for emission from exoplanets located in the Upper Scorpius subgroup of the Sco Cen OB2 Association, the closest substantial region of recent star formation. This survey is different from previous efforts in that it is the first to target exoplanets orbiting Myr-old stars. Young exoplanet systems are expected to be the best candidates for radio detections given the higher magnetic field strengths predicted for young planets as well as the stronger and more dense stellar wind expected for the host stars. The radio emission from exoplanets is expected to be highly circularly polarized therefore we restricted our search to the circular polarization images rather than the total intensity images. We carried out two different search methods using this data. The first method was a targeted search for exoplanet emission using catalogues of known stars and Hot Jupiters within the Upper Scorpius field. The second search method was a blind search for highly circularly polarized sources in the field and for sources identified only in our polarization images. Both the blind and targeted search resulted in non-detections with typical 3σ flux density limits of 4–235 mJy over time-scales of 1.87–1000 min. In particular, we place the first limits on low-frequency emission from the Hot Jupiter systems WASP-17 b and K2-33 b. These are the first results from a larger program to systematically search for low-frequency radio emission from planets orbiting young stars.

Key words: radio continuum: planetary systems.

1 INTRODUCTION

Planets capable of generating strong, planetary-scale magnetic fields are expected to produce bright radio emission (Winglee, Dulk & Bastian 1986; Zarka et al. 2001). The magnetized planets in our own Solar system are known to emit intense, low-frequency radio emission from their auroral regions through the electron-cyclotron maser instability (CMI). This emission arises from the propagation of energetic (keV) electrons along converging magnetic field lines in the planet's magnetosphere. The source of the electron acceleration is an interaction between the solar wind and the planet's magnetosphere. CMI emission is bright, highly beamed, 100 per cent circularly polarized, and sporadic with variability on time-scales ranging from seconds to days (Wu & Lee 1979; Treumann 2006). Analogously, magnetized exoplanets are expected to be sources of bright, low-frequency radio emission (e.g. Winglee et al. 1986; Zarka et al. 2001).

There are over 3000 confirmed exoplanets (Schneider et al. 2011), most of which were discovered through indirect means involving a search for the exoplanet's influence on its host star. Due to the large contrast in brightness between the exoplanet and the host star, far fewer of the known exoplanets have been discovered through direct imaging (Perryman 2011). In contrast, radio emission from magnetized exoplanets is expected to exceed the emission of the planetary host star (Grießmeier et al. 2005) and radio observations could provide another method of direct detection of exoplanets. Radio observations would also provide a direct measurement of the planet's surface magnetic field strength and, in turn, provide insight into the interior composition of these planets. Furthermore, Hess & Zarka (2011) show that the variability of the radio emission in both time and frequency can provide constraints on the rotational period of the planet, the orbital period and inclination and the magnetic field tilt relative to the rotation axis.

Theoretical estimates of the main characteristics of planetary radio emission can be used to select the best targets for observations. Both the expected radio flux density and the emission frequency need to be considered when choosing potential targets. The 'Radiometric Bode's law' is an empirical relation, based on observations

⋆ E-mail: clynch@physics.usyd.edu.au

of the magnetized Solar system planets, that is primarily used to predict the intensity of radio emission from exoplanet systems. This relation relates the incident Poynting or kinetic energy flux of the Solar wind to the radio power produced by a planet (Desch & Kaiser 1984; Zarka et al. 2001). Note that this relation does not mean that auroral radio emission produced by all planets is primarily driven by the stellar wind. For example, the auroral emission observed from Jupiter is mainly driven by its rotation and not the Solar wind (de Pater & Lissauer 2015).

In the last few years there have been a number of theoretical studies that have estimated the expected radio flux densities from exoplanet systems using the Radiometric Bode's law. Farrell, Desch & Zarka (1999) focused on five Solar-like stars with Jupiter systems, finding τ Bootes to be an optimal target. Lazio et al. (2004) expanded on this work and modelled the radio flux density for over 100 sources, noting that planets with small orbital distances should produce mJy level emission. Further work by Stevens (2005) and Grießmeier et al. (2005) focused on investigating the effect the stellar wind and mass loss rate have on the expected flux density. The results from their modelling find that, in the case of kinetic energy-driven Radiometric Bode's law, objects with higher mass-loss rates and wind velocities relative to the Sun are more favourable targets for detections of radio emission.

Grießmeier, Zarka & Spreeuw (2007) compared the kinetic and magnetic energy models for a planet–star interaction. They argued that while the magnetic energy Radiometric Bode's law produces a higher radio flux density, both energy input models need to be considered since it is not clear which dominates in planet–star systems. This idea is supported by the work of Zarka (2007), who found that for the Solar system planets it is not possible to determine which incident power, magnetic or kinetic, drives the CMI emission.

Many of these authors note that precise modelling of the stellar wind is crucial for estimating accurate radio flux densities. This is because the emitted radio power predicted using the Radiometric Bode's law is heavily dependent on the stellar wind parameters. Three dimensional numerical simulations of the stellar winds of both Solar-like stars (Vidotto et al. 2015) and pre-main-sequence stars (Vidotto et al. 2010) have been used to estimate the emitted radio power from Hot Jupiter systems. These efforts suggest that Hot Jupiters orbiting young stars are the best candidates for radio detections if the Radiometric Bode's law holds for all planets.

Counter to the above efforts, Nichols (2011, 2012) suggest that radio emission from some exoplanets may not be dominated by the star–planet interaction and therefore the intensity of the expected radio emission would not follow the Radiometric Bode's law. Rather these planets may generate their auroral emission in a similar manner to Jupiter, through a magnetosphere-ionosphere coupling current system associated with an internal plasma source such as an active moon. In this case, fast-rotating massive planets orbiting in large orbits around XUV-bright stars are capable of generating detectable radio emission. Further arguments against the Radiometric Bode's law suggest that for close-in planets magnetospheric convection will saturate. These systems will not be able to dissipate the total incident stellar wind energy and thus the Radiometric Bode's law will overestimate the flux densities substantially in these cases.

CMI emission occurs near the cyclotron frequency of the emitting electrons,

$$\nu_c = \frac{e B_p}{2\pi m_e} = 2.8 \, B_p \text{ MHz},\tag{1}$$

where m_e and e are the electron mass and charge and B_p is the local polar planetary magnetic field strength in units of Gauss (Farrell et al. 1999). Note for a dipolar magnetic field, B_p is equivalent to twice the equatorial field at a fixed radial distance. Thus, planetary CMI emission is expected to have a high-frequency cut-off related to regions of maximum magnetic field strength near the surface of the planet. This means that predicting the magnetic field strength of potential exoplanet targets is important for determining, which can be observed with current low-frequency telescopes. There are currently two different theoretical approaches for determining the magnetic field of an exoplanet. Grießmeier et al. (2004) and Farrell et al. (1999) use the balance between the Coriolis force, Lorentz force, buoyancy and pressure gradient forces to calculate the planetary magnetic moment and find that it strongly depends on the rotation rate of the planet. The second method of estimating a planet's magnetic field relates the amount of energy flux available from the planet's core to the magnetic field strength. This method finds that the field strength has no dependence on the rotation of the planet and favours young Hot Jupiters (Christensen, Holzwarth & Reiners 2009).

The first non-targeted searches for radio emission from exoplanets occurred before the first detection of the currently known population of exoplanets (Winglee et al. 1986). More recently, searches have involved targeting nearby Hot Jupiters previously detected through radial velocity and transiting observations. Despite the numerous searches for radio emission from exoplanets there have been no unambiguous detections to date (e.g. Bastian, Dulk & Leblanc 2000; Lazio et al. 2004, 2010; George & Stevens 2007; Smith et al. 2009; Stroe, Snellen & Röttgering 2012; Hallinan et al. 2013; Lecavelier des Etangs et al. 2013; Sirothia et al. 2014; Murphy et al. 2015). These attempts rely on the results of optical techniques that tend to be biased towards exoplanet systems around main-sequence stars (Crockett et al. 2012; Lagrange et al. 2013; Johns-Krull et al. 2016). However, from modelling results using the Radiometric Bode's law, its possible that the best targets are Hot Jupiters around pre-main-sequence stars since their stellar winds and mass-loss rates are much greater (Grießmeier et al. 2005; Vidotto et al. 2010).

The Upper Scorpius Association is a region of young stars with ages ranging from 10 to 20 Myr, and is an ideal region to look for radio emission from young exoplanets. This is the closest region with recent star formation, located at a distance of 145 pc, and is thought to contain a few thousand forming stars (de Zeeuw et al. 1999). It is unknown what fraction of forming stars host Hot Jupiter systems, but for Solar-type main-sequence stars about 1 per cent host Hot Jupiter systems (Wright et al. 2012). So we naively expect ∼10 Hot Jupiters in the Upper Scorpius Association, if migration of Hot Jupiters is contemporaneous with gas disc dispersal. Some recent work suggests that Hot Jupiters may migrate to their close orbits after time periods of order 100 Myr, due to planet–planet scattering or Kozai–Lindov resonances (e.g. Knutson et al. 2014). Some giant planets certainly migrate at very young ages (Mann et al. 2016), but the lack of a population of transiting higher mass giant planets hints that a significant fraction of Hot Jupiters may migrate significantly after gaseous disc dispersal. A dominant late migration scenario for Hot Jupiter formation would produce a paucity of radio-bright young Hot Jupiters. We targeted the Upper Scorpius Association with the Murchison Widefield Array (MWA; Tingay et al. 2013). The MWA has a field of view of 144 deg^{-1}, which allowed us to do a blind search of several hundred objects simultaneously. This is the first radio survey to target young exoplanets around forming stars. By targeting a region of best candidates rather than relying on

previous detections in other wavebands, we can avoid any biases or selection effects in those wavebands.

2 OBSERVATIONS AND DATA REDUCTION

We observed the Upper Scorpius Association at 154 MHz, averaging over the full 30.72 MHz bandwidth of the MWA. The observations were carried out between 2015 June 1 and 5. We observed for between 7.3 and 7.6 h per night, for a total of 37.82 h. These observations were recorded as a set of scans with a duration of 1.87 min (or 1.87 min). Each observation scan was reduced and imaged as outlined below.

To calibrate the set of observations for each night, we additionally observed 3C444, a bright calibration source with well-modelled emission, for 1.87 min each night. This source was used to produce a time-independent, frequency-dependent amplitude and phase calibration solution that was applied to the rest of that nights two minute scans. For each scan the visibilities were pre-processed using the COTTER MWA preprocessing pipeline. This pipeline performs the following tasks: flagging radio-frequency interference using the AOFLAGGER (Offringa, van de Gronde & Roerdink 2012), averages the data, and converts the data into a CASA measurement set. Each of the 1.87 min scans was then imaged using the WSCLEAN algorithm (Offringa et al. 2014). For the imaging a pixel size of 0.75 arcsec and image size of 3072 pixels was used. For each 1.87 min scan, we produced a total intensity, Stokes I, image with Briggs weighting of −1 (closer to uniform weighting) and a circular polarization, Stokes V, image with Briggs weighting of +1 (closer to natural weighting). The WSCLEAN algorithm produces these two images by forming a 2×2 complex Jones matrix I for each image pixel. A primary beam correction was performed by inverting the beam voltage matrix B and computing $B^{-1} I B^{*-1}$, where $*$ denotes the conjugate transpose [for further details see Offringa et al. (2014)].

Analysis of the full set of 1.87 min images across all five nights of observations showed that the flux densities for the sources in both Stokes I and V images were severely affected at low elevations. This is due to the foreshortening of the projected baselines at low elevations resulting in beam elongation in the NS direction. To avoid false detections in our Stokes V images at low elevations, we removed the first and last 50 images for each night of observation. This left us with 100 images for a total of 3.3 h per night. For these images, we checked the flux calibration with that of the recently published Galactic and Extragalactic All-sky MWA survey (Hurley-Walker et al. 2017). We find that the flux density scaling is within a factor of 2 of this survey, which is acceptable for the following analysis.

2.1 Median images

The expected flux density of an exoplanet source is less than a few tens of mJy and so to achieve the required sensitivities we median stacked our 1.87 min images to create images covering longer integrations. We did not need to regrid the 1.87 min images as they are already on a common coordinate grid, centred at an RA and Dec. of 240°.0, −30°.0 . We chose to use the median of the pixel values rather than the mean because the mean is more sensitive to poor quality images.

Before stacking our images, we needed to take into account the variability time-scale expected for planetary emission. Due to the narrow beaming of the expected CMI emission, radio emitting planets will only be detected over ranges of rotational and orbital phases during which their active magnetic field lines are suitably oriented relative to our line of sight. Further, Hess & Zarka (2011) simulated

Table 1. Measured 3σ noise limits for images over different time-scales.

Image	Time (min)	Stokes I (mJy)	Absolute Stokes V (mJy)	Stokes V (mJy)
Snapshot	1.87	235	110	110
Hourly	60	68	37	20
Nightly	200	46	31	12
Full Data set	1000	39	30	4

the expected dynamic spectra for Hot Jupiter systems and showed that the detectable emission covers only a few percent of the rotational or orbital phase. Because the rotational period of exoplanets are unknown and exoplanets orbiting close (<0.1 au) to the host star are expected to be tidally locked (Grießmeier et al. 2004), we assume the rotational period of the potentially detected Hot Jupiters to be the same as their orbital period. The majority of the currently known Hot Jupiter systems have orbital periods between 1 and 6 d (Schneider et al. 2011). From the simulated dynamic spectra of Hess & Zarka (2011), we assume the emission lasts up to five per cent of the orbital phase and consequently, we expect to see variability on time-scales of 1–7 h. To take into account this variability, we median-stacked the 1.87 min images to create images on two time-scales: hourly and nightly. We also stacked all 500 of the remaining images to produce a single deep image and place the best upper limits on the expected radio flux density in the case of non-detections.

Furthermore, we need to also consider the possibility of polarization reversal. CMI emission can either be left or right-handed circularly polarized depending on the hemisphere from which it is emitted (Zarka 1998; Lamy et al. 2008). Thus, the polarization of the emission observed with the MWA will be dependent on which hemisphere is visible to the telescope and can change with either the planet rotation or orbit, as shown by Hess & Zarka (2011). Polarization helicity reversal has been observed in other sources of CMI emission (e.g. ultracool Dwarfs: Hallinan et al. 2007; Lynch, Mutel & Güdel 2015) and should be considered when stacking Stokes V images. To avoid depolarizing our images through stacking over opposite helicities, we two sets of Stokes V median stack images, one in which we take the absolute value of all the pixels before creating the median stack images in Stokes V.

The average sensitivity achieved in each of the stacked images is listed in Table 1, including both cases of Stokes V stacking (absolute values and not). To estimate the noise in each image, we use the 99.7 percentile of the pixel distributions (equivalent to a 3σ limit). Due to the compactness of the MWA, it has been shown that the noise in the Stokes I images will be dominated by classical and side-lobe confusion (Franzen et al. 2016; Rowlinson et al. 2016). The Stokes I rms values, we measure are consistent with these previous studies. Due to the much smaller number of sources with circular polarization, our Stokes V images are not confusion limited. The noise in these images is expected to be dominated by thermal noise of the telescope. However, stacking the absolute value of the pixels causes the final stacked Stokes V images to be somewhat less sensitive than expected. Comparing to the rms noise for median stacked images without using the absolute pixel values, the noise is increased in our images by a factor of 1.85 for the 60 min images, 2.58 for 200 min images and 7.5 for the 1000 min image. The median stack of the absolute pixel-values is clearly not the optimal statistic to use for combining these images and further work is needed to determine what is the best way to combine images to increase the sensitivity without reducing the polarized signal.

3 SEARCHING FOR EXOPLANETS

For each set of images (hourly, daily and full observation), we used the source finder AEGEAN (Hancock et al. 2012) with a 5σ detection threshold to create catalogues of significant sources within the Stokes I and V images. Due to the imperfect MWA primary beam model, the flux density measurements far from the phase centre of the observation can have errors of up to 10 per cent (Hurley-Walker et al. 2014); with this in mind we restrict our search to sources located within the primary beam of the image or within a distance of $12°$ from the phase centre. These three sets of catalogues were then used to carry out two different methods to search for exoplanet emission in the images. Since CMI emission from planetary systems is known to be highly circularly polarized (Wu & Lee 1979; Treumann 2006), in this analysis we focus solely on the circularly polarized sources. This has the added benefit that our Stokes V images are more sensitive than our Stokes I images (see Table 1).

3.1 Targeting known sources within the field

We carried out a targeted search for exoplanet emission using catalogues of known stars and exoplanets within the Upper Scorpius field. For each of the catalogues we first cross-matched the catalogue with our two catalogues (absolute and normally stacked) of Stokes V sources in the hourly, daily and full median stack images. Using the results of that cross-match, we then carry out a second cross-match with the Stokes I catalogues and calculate the fractional polarization for sources common to both Stokes catalogues. We then investigate those sources with fractional polarization greater than 0.5. Because our Stokes I images are less sensitive that our Stokes V images, we also investigate sources which only have matches in our Stokes V catalogues.

While the Sco Cen OB2 Association is nearby, the identification of stars within this association is not complete for most mass regimes. The exception is for the most massive stars, whose membership has been fully characterized by Rizzuto, Ireland & Robertson (2011). They identify 436 high mass members located within Sco Cen OB2. There are expected to be ~2000 pre-main-sequence late K- and M-type stars located within the Upper Scorpius (Preibisch et al. 2002). Rizzuto, Ireland & Kraus (2015) have started to characterize this population of stars and identify 237 spectroscopically confirmed stars in Upper Scorpius. Combining these two catalogues, we have the most complete known census of the stellar population within Upper Scorpius. We use the location of these objects in our targeted search as potential hosts for exoplanet systems. Additionally, we use the Extrasolar Planetary Encyclopedia (Schneider et al. 2011) to identify two Hot Jupiter systems located within the field: K2-33 b (David et al. 2016; Mann et al. 2016) and WASP-17 b (Anderson et al. 2010). We list the relevant physical parameters measured for these two systems in Table 2, including the distance to the system, d, the mass, M_p, and radius, R_p of the planet, the semimajor axis of the planet's orbit, a, and the age, t, of the host star.

3.1.1 Hot Jupiter Systems K2-33 b and WASP-17 b

The two known Hot Jupiter systems were not associated with any of the Stokes V sources in our catalogues over any of the time-scales. Fig. 1 shows the 16.6 h median stack Stokes V image overlaid with the Stokes I contours for WASP-17 and K2-33b. The best limit on the Stokes V emission comes from the normally stacked Stokes V image of the full data set. The 3σ upper limits to the 154 MHz

Table 2. Physical Parameters for Hot Jupiters within the Upper Scorpius field as defined in section 3.1.1.

	K2-33 b	WASP-17 b
d (pc)	145	400
M_p (M$_J$)	3.6	0.486
R_p (R$_J$)	0.45	1.991
a (au)	0.041	0.0515
t (Gyr)	0.0095	3.0
$\dot{M}$ (M$_\odot$ yr^{-1})	10^{-9}	4×10^{-14}
$B_{p, G}$ (G)	$[0.8...25.0]^a$	$[0.008...0.03]^a$
$\nu_{c, G}$ (MHz)	$[2.2...70.0]$	$[0.02...0.09]$
$S_{\nu_{c,G}}$ (mJy)	$[11.7...37.0]$	$[0.16...0.26]$
$B_{p, R}$ (G)	124^b	6^b
$\nu_{c, R}$ (MHz)	346	16
$S_{\nu_{c,R}}$ (mJy)	34.0	0.01
S_{154} (mJy)	9.7	8.4

^{a}Using the scaling laws in Grießmeier et al. (2004).
^{b}Using the scaling laws in Reiners, Basri & Christensen (2009).

emission are listed in Table 2 as S_{154}. We estimated this value by measuring the 99.7 percentile of the pixel values within an area several times the resolving beam centred on the location of each source. In this table, we also give the predicted mass-loss rate and magnetic field strengths for both sources, which we use to calculate the expected emission frequency and radio flux density.

For young objects like K2-33, the mass-loss rates are not well constrained by measurements and to estimate of the mass-loss rate for this object we rely on the modelling efforts of Vidotto et al. (2010). Vidotto et al. (2010) use 3D numerical magnetohydrodynamic simulations to study the stellar winds of Myr-old stars that have dissipated their accretion dicks. They estimate a mass-loss rate of 10^{-9} M$_\odot$ yr^{-1} for these young stars. For stars with ages greater than 700 Myr, the mass-loss rates are well modelled by the empirically derived relation $\dot{M} \propto t^{-2.00 \pm 0.52}$, where t is the age of the star (Wood et al. 2002; Lammer et al. 2004). We use this expression to estimate the mass-loss rate for WASP-17. The estimated mass-loss rates, $\dot{M}$, are listed in Table 2.

Depending on the physical parameters of the planet, the two theoretical models developed for predicting magnetic field strengths can differ by factors of 2–5. To get a sense of what range of magnetic field strengths are predicted for these two objects, we calculate the strength of the magnetic field using both methods. Grießmeier et al. (2004) list four different scaling relations for the magnetic moment of a planet which depend on the mass, radius and rotation rate of the planet. Assuming WASP-17 b and K2-33 b are tidally locked to their host star and following exactly the procedure outlined in Grießmeier et al. (2004), we calculate the range of magnetic field strengths $B_{p, G}$ in Table 2. We use the scaling law by Reiners et al. (2009) to calculate a second set of magnetic field strengths. This expression depends on the mass, radius and luminosity of the planet. Both the mass and radius for each of these planets is already known and so we use the evolutionary tracks calculated by Burrows et al. (1993, 1997) to estimate the luminosities for each planet. Using these values, we calculate the magnetic field strengths $B_{p, R}$ in Table 2. We also list the associated maximum cyclotron frequency, ν_c, that we expect given these field strengths.

Using the different sets of field strengths and mass-loss rates, we can use the expressions derived by Grießmeier et al. (2005) for the predicted radio flux density emitted by a planet:

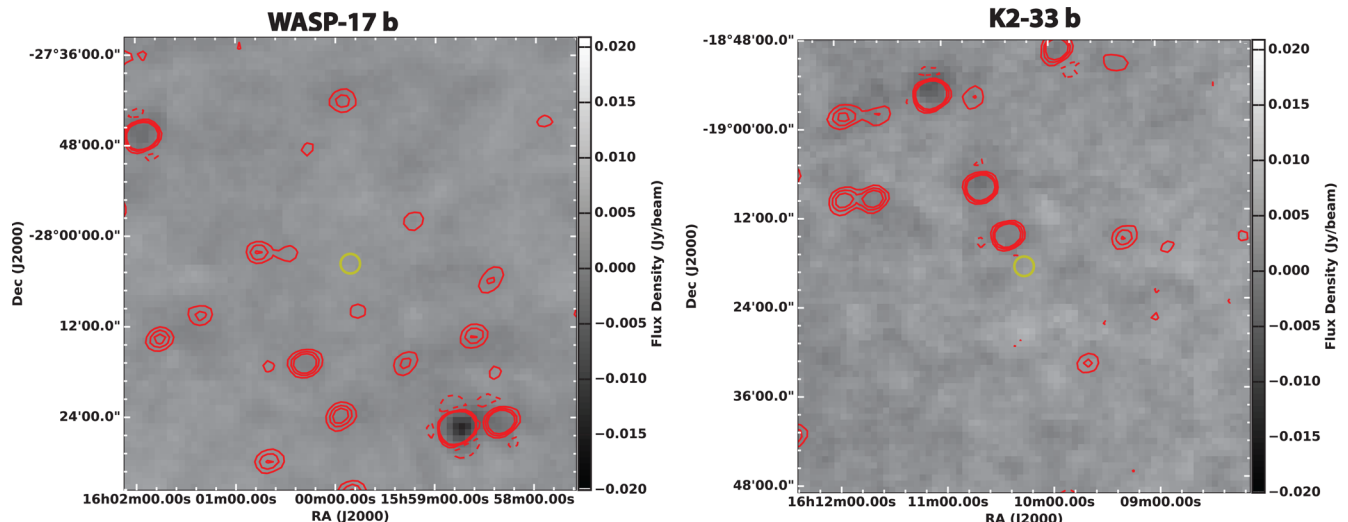$$S_\nu \propto R_p^3\, \mu^{-1/3}\, n_0^{2/3}\, \nu^{7/3} d^{-4/3} \tag{2}$$

Figure 1. The 154 MHz Stokes V images overlaid with Stokes I contours for the two known Hot Jupiter systems in this field: WASP-17 b (left-hand panel) and K2-33 b (right-hand panel); the yellow circle marks the location of each source in their respective image. Both the contours and images are the result of the 16.6 h median stack. The contour levels are $-1, 1, 2, 3$ times 39.0 mJy, the Stokes I 3σ noise value.

This expression assumes the case of kinetic energy dominate Radiometric Bode's law. We first re-write equation (2) in terms of the stellar mass-loss rate, $n_0 \propto \dot{M}/v$ and planetary magnetic field, $B \propto \mu/R_p^3$:

$$S_\nu \propto R_p^2 \, B_p^{-1/3} \, \dot{M}^{2/3} \, v^{5/3} \, a^{-4/3} d^{-2}, \qquad (3)$$

where μ is the magnetic moment for a planet with magnetic field strength B_p, radius R_p and semimajor axis a, $\dot{M}$ is the mass-loss rate for a star with stellar wind velocity v and density n_0, located at a distance of d. We then scale all of the physical parameters in terms of Jupiter's physical parameters and note that Jupiter has an average flux density of $\Phi_J = 5.1 \times 10^7$ Jy at 1 au. By scaling this relation in terms of Jupiter, we are assuming that Jupiter's radio emission can be described by the Radiometric Bode's law. This may not be true as the radio emission from Jupiter is not primarily driven through energy injection by the Solar wind but by the planet's rotation. Further, in using the Radiometric Bode's law, we are assuming that both K2−33 B and WASP−17 b are able to convert all of the stellar wind energy flux into radio power.

The predicted flux densities for both of the known Hot Jupiter systems are listed in Table 2. The predicted magnetic field strength and flux density of WASP−17 b are not favourable for our MWA observation since the maximum frequency is less than 150 MHz, and the expected flux density would be difficult to detect even with the most sensitive of today's low-frequency telescopes. Note that if the magnetic field strength of WASP−17 b is best described by the scaling relations in Grießmeier et al. (2004), the maximum frequency would be too low to be able to detect using ground-based telescopes since its below the 10 MHz ionospheric cut-off frequency. Owing to its young age and high mass, K2−33 b has much better predicted values for both the emission frequency and radio flux density. In Section 4, we discuss some reasons why we did not detect any emission from this source.

3.1.2 Young Stars

We do not detect any sources with fractional circular polarization greater than 0.5 in either of the sets of stacked Stokes V images for both the Rizzuto et al. (2011) and Rizzuto et al. (2015) catalogues.

We found one source in the Rizzuto et al. (2011) catalogue to be associated with only Stokes V emission in the absolute value stacked Stokes V image on hourly time-scales. We created $1° \times 1°$ postage-stamp images for this source in Stokes I and v to further investigate this emission. We found that the source of stokes v emission is associated with leakage due to a Stokes I beam artefact from nearby bright source.

3.2 Blind search within the field

To carry out a blind search for exoplanet emission, again we focus solely on Stokes V emission. First, we cross-matched the Stokes I and V catalogues for each image to find sources with fractional polarization greater than 0.5. Once more, we did not find any sources on any time-scale with fractional polarization >0.5 for either set of stacked Stokes V images. We then investigated sources in each of the images that were not associated with any of the Stokes I sources. For the absolute value stacked images, we did not find any sources associated with only Stokes V emission on any time-scale. For the normal stacked Stokes V images, we found on hourly time-scales there were two sources, on nightly time-scales two sources, and in the full median stack there were no sources. Again, we created $1° \times 1°$ postage-stamp images for each of these sources to visually inspect the emission. Upon inspection of the Stokes V sources in the $1° \times 1°$ postage-stamp images, all four of the sources were found to be associated with leakage from a beam artefact from a nearby source.

4 DISCUSSION AND CONCLUSIONS

We used the MWA to observe the Upper Scorpius Association over five consecutive nights in 2015 June. The purpose of these observations was to look for 154 MHz emission from young Hot Jupiter systems in this region. This is the first radio survey to target a region of young stars to look for exoplanets. We restricted our search to the Stokes V images of Upper Scorpius because the exoplanet emission is believed to be almost 100 per cent circularly polarized. This has the added benefit of the circularly polarized images having better sensitivity than the total intensity images. In this search,

we targeted known stars that could host an exoplanet system as well as two known Hot Jupiters systems, WASP-17 b and K2-33 b. Additionally, we did a blind search for sources with high fractional circular polarization and sources identified only in our Stokes V images. Both the targeted and blind searches resulted in non-detections and we place the first limits on the radio emission from WASP-17 b and K2-33 b.

While the flux density and magnetic field strength predicted for the Solar-age WASP-17 b are too low to be detected by the MWA, the flux density and field expect for the much younger K2-33b are within the detection limits of this telescope. To determine whether known exoplanet systems are likely to lie within the flux density and frequency limits of the MWA, we use the Extrasolar Planetary Encyclopaedia to identify 682 exoplanet systems with $a \leq 5.2$ au and calculate the expected radio flux density and maximum observing frequency for each source using the relevant information. We find that 10 out of the 682 sources, or 1 per cent of these objects, are within the sensitivity and frequency limits of the MWA. As noted before, the majority of these objects have ages ≥ 1 Gyr. Selecting sources with ages <1 Gyr, 6 of the remaining 43 sources, or 14 per cent, are within the sensitivity and frequency limits of the MWA. So we expect a small portion of unknown young Hot Jupiters within this field to have flux densities and field strengths within the limits of the MWA. There is several possible reason why we didn't detect any exoplanets in this field.

The first reason is that we could have overestimated the expected flux density from Hot Jupiters in this field. Modelling efforts throughout the literature provide a wide range of expected flux densities. In fact, those by Grießmeier, Zarka & Girard (2011) are about an order of magnitude higher than ours. These differences are mainly due to the poorly constrained stellar wind velocity close to the host star, in a region where the wind has yet to reach its terminal velocity. Vidotto et al. (2010) point-out that many models overestimate the expected flux density because they assume the terminal velocity of the wind. Without having better constraints on the wind parameters the order of magnitude uncertainties in the radio flux density estimates will remain.

Further, in our modelling we assume the emission is driven by the kinetic energy Radiometric Bode's law, but its possible that the magnetic case may dominate in most cases. Grießmeier et al. (2007) estimate flux densities of the order of 10 mJy for the situation of magnetic energy dominate planet–star interaction. This would be challenging to detect with the MWA. Even worse still, Nichols & Milan (2016) argue that due to the saturation of magnetosphereic convection for Hot Jupiters, these systems will not be able to dissipate the total incident magnetic energy. Thus the magnetic Radiometric Bode's law over estimates the flux densities substantially. Nichols & Milan (2016) calculate flux densities of the order of 1 mJy in the case of convection saturation. Future low-frequency telescopes, like the Square Kilometre Array (Lazio et al. 2009), will have better sensitivity and could make a detection if the flux densities are an order of magnitude lower.

A second issue is that we may have overestimated the magnetic field strength and thus the maximum frequency of the radio emission. The scaling laws in Grießmeier et al. (2004) predict magnetic field strengths much lower than those of Reiners et al. (2009). For example, the magnetic fields estimated for K2-33 b using Grießmeier et al. (2004) are associated with maximum frequencies that are undetectable with the MWA. It is currently not known which relations, those in Grießmeier et al. (2004) or Reiners et al. (2009), more accurately predict the magnetic field strength of a given planet. However,

a radio detection would be one way to discriminate between these two models.

The last issue, we would like to address is the beaming of the radio emission. Radio emission from exoplanets is most likely orbitally beamed. This is seen in other objects known to produce CMI emission, such as the Solar system planets and ultracool dwarfs. For orbital periods between 1 and 6 d, our 16.6 h of total observation only covers between 11 and 60 per cent of these orbital periods. Furthermore, the inclination of the planetary rotation axis and the orbital axis of the system will determine whether the beam of emission sweeps in the direction of the Earth. For example, Hess & Zarka (2011) find that for inclinations of the planetary orbital plane $\geq 60°$ no emission is detectable independent of the inclination angle of the magnetic axis. If we only expect ~10 Hot Jupiters in this field it is possible that a combination of unfavourable orbital geometry and lacking full orbital coverage could have prevented us from detecting exoplanetary 154 MHz emission. To mitigate these problems, constant monitoring of a large number of young stars could ensure, we observe objects with favourable geometries during orbital phases that sweep emission in the direction of the Earth.

In the future, we plan to carry out similar MWA observing campaigns of other nearby star-forming regions. By monitoring large samples of young stars in these regions, we can build up a census of transit phenomena in these regions and target the best candidates to lead to a radio detection of an exoplanet.

REFERENCES

Anderson D. R. et al., 2010, ApJ, 709, 159
Bastian T. S., Dulk G. A., Leblanc Y., 2000, ApJ, 545, 1058
Burrows A., Hubbard W. B., Saumon D., Lunine J. I., 1993, ApJ, 406, 158
Burrows A. et al., 1997, ApJ, 491, 856
Christensen U. R., Holzwarth V., Reiners A., 2009, Nature, 457, 167
Crockett C. J., Mahmud N. I., Prato L., Johns-Krull C. M., Jaffe D. T., Hartigan P. M., Beichman C. A., 2012, ApJ, 761, 164
David T. J. et al., 2016, Nature, 534, 658
de Pater I., Lissauer J. J., 2015, Planetary Sciences. Cambridge Univ. Press, Cambridge
de Zeeuw P. T., Hoogerwerf R., de Bruijne J. H. J., Brown A. G. A., Blaauw A., 1999, AJ, 117, 354
Desch M. D., Kaiser M. L., 1984, Nature, 310, 755
Farrell W. M., Desch M. D., Zarka P., 1999, J. Geophys. Res., 104, 14025
Franzen T. M. O. et al., 2016, MNRAS, 459, 3314
George S. J., Stevens I. R., 2007, MNRAS, 382, 455

Grießmeier J.-M. et al., 2004, A&A, 425, 753

Grießmeier J.-M., Motschmann U., Mann G., Rucker H. O., 2005, A&A, 437, 717

Grießmeier J.-M., Zarka P., Spreeuw H., 2007, A&A, 475, 359

Grießmeier J.-M., Zarka P., Girard J. N., 2011, Radio Sci., 46, RS0F09

Hallinan G. et al., 2007, ApJ, 663, L25

Hallinan G., Sirothia S. K., Antonova A., Ishwara-Chandra C. H., Bourke S., Doyle J. G., Hartman J., Golden A., 2013, ApJ, 762, 34

Hancock P. J., Murphy T., Gaensler B. M., Hopkins A., Curran J. R., 2012, MNRAS, 422, 1812

Hess S. L. G., Zarka P., 2011, A&A, 531, A29

Hurley-Walker N. et al., 2014, PASA, 31, e045

Hurley-Walker N. et al., 2017, MNRAS, 464, 1146

Johns-Krull C. M. et al., 2016, ApJ, 826, 206

Knutson H. A. et al., 2014, ApJ, 785, 126

Lagrange A.-M., Meunier N., Chauvin G., Sterzik M., Galland F., Lo Curto G., Rameau J., Sosnowska D., 2013, A&A, 559, A83

Lammer H., Ribas I., Grießmeier J.-M., Penz T., Hanslmeier A., Biernat H. K., 2004, Hvar Obs. Bull., 28, 139

Lamy L., Zarka P., Cecconi B., Prangé R., Kurth W. S., Gurnett D. A., 2008, J. Geophys. Res., 113, A07201

Lazio W. T. J., Farrell W. M., Dietrick J., Greenlees E., Hogan E., Jones C., Hennig L. A., 2004, ApJ, 612, 511

Lazio J. et al., 2009, Astro2010: The Astronomy and Astrophysics Decadal Survey, Science White Papers, 177.

Lazio T. J. W., Shankland P. D., Farrell W. M., Blank D. L., 2010, AJ, 140, 1929

Lecavelier des Etangs A., Sirothia S. K., Gopal-Krishna, Zarka P., 2013, A&A, 552, A65

Lynch C., Mutel R. L., Güdel M., 2015, ApJ, 802, 106

Mann A. W. et al., 2016, AJ, 152, 61

Murphy T. et al., 2015, MNRAS, 446, 2560

Nichols J. D., 2011, MNRAS, 414, 2125

Nichols J. D., 2012, MNRAS, 427, L75

Nichols J. D., Milan S. E., 2016, MNRAS, 461, 2353

Offringa A. R., van de Gronde J. J., Roerdink J. B. T. M., 2012, A&A, 539, A95

Offringa A. R. et al., 2014, MNRAS, 444, 606

Perryman M., 2011, The Exoplanet Handbook, 1st edn. Cambridge Univ. Press, Cambridge

Preibisch T., Brown A. G. A., Bridges T., Guenther E., Zinnecker H., 2002, AJ, 124, 404

Reiners A., Basri G., Christensen U. R., 2009, ApJ, 697, 373

Rizzuto A. C., Ireland M. J., Robertson J. G., 2011, MNRAS, 416, 3108

Rizzuto A. C., Ireland M. J., Kraus A. L., 2015, MNRAS, 448, 2737

Rowlinson A. et al., 2016, MNRAS, 458, 3506

Schneider J., Dedieu C., Le Sidaner P., Savalle R., Zolotukhin I., 2011, A&A, 532, A79

Sirothia S. K., Lecavelier des Etangs A., Gopal-Krishna Kantharia N. G., Ishwar-Chandra C. H., 2014, A&A, 562, A108

Smith A. M. S., Collier Cameron A., Greaves J., Jardine M., Langston G., Backer D., 2009, MNRAS, 395, 335

Stevens I. R., 2005, MNRAS, 356, 1053

Stroe A., Snellen I. A. G., Röttgering H. J. A., 2012, A&A, 546, A116

Tingay S. J. et al., 2013, PASA, 30, e007

Treumann R. A., 2006, A&A Rev., 13, 229

Vidotto A. A., Opher M., Jatenco-Pereira V., Gombosi T. I., 2010, ApJ, 720, 1262

Vidotto A. A., Fares R., Jardine M., Moutou C., Donati J.-F., 2015, MNRAS, 449, 4117

Winglee R. M., Dulk G. A., Bastian T. S., 1986, ApJ, 309, L59

Wood B. E., Müller H.-R., Zank G. P., Linsky J. L., 2002, ApJ, 574, 412

Wright J. T., Marcy G. W., Howard A. W., Johnson J. A., Morton T. D., Fischer D. A., 2012, ApJ, 753, 160

Wu C. S., Lee L. C., 1979, ApJ, 230, 621

Zarka P., 1998, J. Geophys. Res., 103, 20159

Zarka P., 2007, Planet. Space Sci., 55, 598

Zarka P., Treumann R. A., Ryabov B. P., Ryabov V. B., 2001, Ap&SS, 277, 293

This paper has been typeset from a TEX/LATEX file prepared by the author.